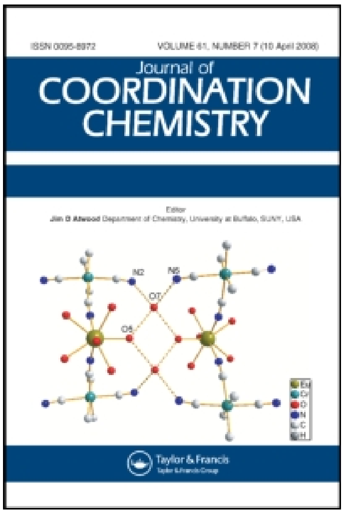

Journal of Coordination Chemistry
Publication details, including instructions for authors and subscription information:
http://www.informaworld.com/smpp/title~content=t713455674

Two 2-D lanthanide coordination polymers constructed from hydroquinone-O,O'-diacetic acid

Xia Li[a]; Yanqiu Li[a]; Yanbing Zhang[a]
[a] Department of Chemistry, Capital Normal University, Beijing, China

To cite this Article Li, Xia , Li, Yanqiu and Zhang, Yanbing(2008) 'Two 2-D lanthanide coordination polymers constructed from hydroquinone-O,O'-diacetic acid', Journal of Coordination Chemistry, 61: 11, 1720 — 1729
To link to this Article: DOI: 10.1080/00958970701747038
URL: http://dx.doi.org/10.1080/00958970701747038

Journal of Coordination Chemistry
Vol. 61, No. 11, 10 June 2008, 1720–1729

Taylor & Francis
Taylor & Francis Group

Two 2-D lanthanide coordination polymers constructed from hydroquinone-O,O′-diacetic acid

XIA LI*, YANQIU LI and YANBING ZHANG

Department of Chemistry, Capital Normal University, Beijing, China

(*Received 8 May 2007; in final form 15 June 2007*)

Two new coordination polymers, $\{Ln_2(hqda)_3(H_2O)_4{\cdot}6H_2O\}_n$ (H_2hqda = hydroquinone-O,O′-diacetic acid, Ln = Dy, **1**; Ho, **2**), were prepared and characterized by elemental analysis, IR spectroscopy, TG-DTA, fluorescence spectroscopy, and single-crystal X-ray diffraction. The two complexes are isomorphous with similar crystal structures. In **1** and **2**, each Ln(III) ion is nine coordinate with seven oxygen atoms from hqda ligands and two oxygen atoms from water molecules. Two adjacent Ln(III) ions are bridged by $–COO^-$ groups from hqda ligands in bidentate-bridging and chelating-bridging modes. These building blocks cross link through $^-OOCCH_2OC_6H_4OCH_2COO^-$ spacers to form a 2–D network structure. The adjacent 2-D layers are further interlinked by hydrogen bonds to form a 3-D supermolecular structure.

Keywords: Lanthanide coordination polymers; Hydroquinone-O,O′-diacetic acid; Crystal structure

1. Introduction

Coordination polymers with metal-organic frameworks (MOFs) have attracted interests owing to both fascinating structures and potential applications in magnetism, catalysis, adsorption, and luminescent probes [1–5]. Lanthanide coordination polymers are of interest because lanthanide ions have larger coordination spheres, unique fluorescence, and magnetic properties [1–12]. Organic ligands are a key for construction of MOFs with open pores of different shapes and sizes. Polycarboxylate ligands construct MOFs with metal ions, because the carboxylate groups adopt rich coordination modes [4–12]. The geometry of the polycarboxylate ligand may influence the MOFs structure. Comparing with widely used benzedicarboxylate ligands [6–11], hydroquinone-O,O′-diacetic acid (H_2hqda) ligand has both flexibility and rigidity. The two carboxyl groups with longer spacers at opposite positions on the benzene ring can form MOFs with diverse sizes and shapes. Therefore, H_2hqda is a good ligand in construction of coordination polymers with open frameworks. There are a few publications about the coordination chemistry of H_2hqda with lanthanides [12], transition metals [13], and alkaline earth metals [14].

---

*Corresponding author. Tel.: +86 10 68902320. Fax: +86 10 68902320. Email: xiali@mail.cnu.edu.cn

Journal of Coordination Chemistry
ISSN 0095-8972 print/ISSN 1029-0389 online © 2008 Taylor & Francis
DOI: 10.1080/00958970701747038

MOFs relate to both the nature of the metal ion as nodes and the organic ligand as spacers. Lanthanide complexes with carboxylate are prepared by hydrothermal, conventional solution reaction, sol gel diffusion, and solution diffusion methods. Using different synthetic methods may lead to diversity of MOFs. The hydrothermal synthesis approach has been successful in many systems of lanthanide polycarboxylate coordination polymers, including two lanthanide H_2hqda coordination polymers, $[Eu_2(1,4\text{-BDOA})_3(H_2O)_2] \cdot 2H_2O$ and $[Er_2(1,4\text{-BDOA})_3(H_2O)_2]$ (1,4-BDOA = hydroquinone-O,O′-diacetic acid), in which ether oxygen atoms from 1,4-BDOA ligands also coordinate lanthanide ions [12]. The H_2hqda ligand with lanthanide ions using the solution diffusion methods gave two new coordination polymers, $\{Ln_2(hqda)_3(H_2O)_4 \cdot 6H_2O\}_n$ (H_2hqda = hydroquinone-O,O′-diacetic acid, Ln = Dy, **1**; Ho, **2**). In **1** and **2**, ether oxygen atoms from hqda ligands did not coordinate lanthanide ions and resulted in 2–D network structures different from those above.

2. Experimental

2.1. *Materials and methods*

All analytical grade chemicals and solvents were purchased and used without further purification. $LnCl_3 \cdot 6H_2O$ (Ln = Dy, Ho) was made from the reaction of lanthanum oxide (99.90%) and hydrochloric acid.

Elemental analyses (C, H, N) were carried out on an Elementar Vario EL analyzer. IR spectra were recorded on a Bruker Equinox 55 FT-IR spectrometer with KBr pellets at the range of 400–4000 cm^{-1}. Excitation spectrum and emission spectrum of the solid samples were recorded on a F-4500 fluorescence spectrophotometer at room temperature. Thermogravimetric analysis was performed on a WCT-1A thermal analyzer with a heating rate of 10°C/min from 20 to 1000°C.

2.2. *Synthesis of the title complexes*

A solution containing ethanol and a little triethylamine slowly diffused into a DMF-water solution of $LnCl_3 \cdot 6H_2O$ (0.2 mmol) (Ln = Dy and Ho) and H_2hqda (0.3 mmol). Single crystals were obtained after several days. Yield: 52% for **1** and 47% for **2**. For **1**, $C_{15}H_{22}DyO_{14}$ (588.83), Calcd (%): C, 30.60; H, 3.76. Found (%): C, 30.79; H, 3.89. Selected IR (KBr pellet, ν/cm^{-1}): 3424 br, 2923 w, 1579 vs, 1508 vs, 1420 s, 1231 s, 1196 s, 1078 m, 830 m, 776 m, 533 w. For **2**, $C_{15}H_{22}HoO_{14}$ (591.26), Calcd. (%): C, 30.47; H, 3.75. Found (%): C, 30.65; H, 3.68. Selected IR (KBr pellet, ν/cm^{-1}): 3422 br, 2925 w, 1579 vs, 1509 vs, 1422 s, 1231 s, 1199 s, 1079 m, 832 m, 777 m, 534 w.

2.3. *Crystal structure determination*

X-ray single crystal diffractions for **1** and **2** were performed on a Bruker Smart 1000CCD diffractometer with monochromated Mo Kα radiation ($\lambda = 0.71073$ Å) at 293 K. Semi-empirical absorption corrections were applied using the SADABS program. All calculations were carried out on a computer with use of

SHELXS-97 and SHELXL-97 [15, 16]. The structures were solved by direct methods and refinement on $|F|^2$ used full-matrix least-squares methods. Summary of the crystallographic data and details of the structure refinements are listed in table 1. Selected bond lengths and angles of **1** and **2** are listed in tables 2 and 3, respectively.

3. Results and discussion

3.1. *Structural description of complexes*

The asymmetric unit of **1** containing two Dy(III) ions is shown in figure 1. Two bidentate-bridging COO^- groups (O1–C1–O2 and O1A–C1A–O2A) and two chelating-bridging COO^- groups (O5B–C10B–O6B and O5C–C10C–O6C) from hqda ligands link neighboring Dy(III) ions to form a dimeric unit with central symmetry; the distance between Dy1 and Dy1A is 3.885(5) Å. The Dy1(III) ion is nine coordinate by seven oxygen atoms of hqda ligands and two oxygen atoms of water. The coordination environment of Dy(III) can be described as a distorted monocapped square antiprism. Atoms O2A, O6C, O8, O11, O1, O5B, O6B, and O10 form the upper and lower squares with mean deviations of 0.172 and 0.085 Å, respectively, and dihedral angle between them of 1.8°. Atom O7 caps the upper plane. The Dy1-O(carboxyl) bond lengths vary

Table 1. Crystal data and structure refinement for **1** and **2**.

Complex	**1**	**2**
Empirical formula	$C_{15}H_{22}DyO_{14}$	$C_{15}H_{22}HoO_{14}$
Formula weight	588.32	591.26
Temperature (K)	294(2)	293(2)
Wavelength (Å)	0.71073	0.71073
Crystal system	Triclinic	Triclinic
Space group	$P\bar{1}$	$P\bar{1}$
a (Å)	8.6146(11)	8.6130(17)
b (Å)	9.6880(12)	9.6681(19)
c (Å)	12.7062(16)	12.711(3)
α (°)	102.527(2)	102.48(3)
β (°)	95.208(2)	95.27(3)
γ (°)	106.691(2)	106.66(3)
V (Å^3)	978.2(2)	976.6(4)
Z	2	2
D_{calcd} (Mg m^{-3})	1.999	2.001
μ (mm^{-1})	3.893	4.125
$F(000)$	580	582
Crystal size (mm^3)	0.20 × 0.16 × 0.12	0.24 × 0.20 × 0.16
θ range for data collection (°)	1.66 to 16.39	2.27 to 28.28
Limiting indices	$-10 \leqq h \leqq 10$	$-11 \leqq h \leqq 11$
	$-12 \leqq k \leqq 9$	$-12 \leqq k \leqq 12$
	$-15 \leqq l \leqq 15$	$-16 \leqq l \leqq 16$
Reflections collected/unique	5662/3941 [R(int) = 0.0168]	17742/4823[R(int) = 0.0173]
Data/restraints/parameters	3941/201/271	4823/0/281
Goodness-of-fit on F^2	1.122	1.083
Final R indices [$I > 2\sigma$(I)]	$R_1 = 0.0240$, $wR_2 = 0.0550$	$R_1 = 0.0135$, $wR_2 = 0.0326$
R indices (all data)	$R_1 = 0.0274$, $wR_2 = 0.0562$	$R_1 = 0.0141$, $wR_2 = 0.0329$
Largest diff. peak and hole (e Å^{-3})	1.415 and −1.462	0.484 and −0.615

Table 2. Bond lengths [Å] and angles [°] for **1**.

Dy(1)–O(10)	2.340(3)	Dy(1)–O(2)#1	2.363(2)
Dy(1)–O(1)	2.367(2)	Dy(1)–O(11)	2.396(3)
Dy(1)–O(6)#2	2.403(2)	Dy(1)–O(8)	2.426(2)
Dy(1)–O(6)#3	2.491(2)	Dy(1)–O(7)	2.501(2)
Dy(1)–O(5)#3	2.546(2)		
O(10)–Dy(1)–O(2)#1	140.39(9)	O(10)–Dy(1)–O(1)	69.93(9)
O(2)#1–Dy(1)–O(1)	138.99(8)	O(10)–Dy(1)–O(11)	70.93(10)
O(2)#1–Dy(1)–O(11)	84.92(9)	O(1)–Dy(1)–O(11)	135.97(9)
O(10)–Dy(1)–O(6)#2	141.70(9)	O(2)#1–Dy(1)–O(6)#2	74.20(8)
O(1)–Dy(1)–O(6)#2	71.80(8)	O(11)–Dy(1)–O(6)#2	142.76(8)
O(10)–Dy(1)–O(8)	82.82(10)	O(2)#1–Dy(1)–O(8)	124.85(8)
O(1)–Dy(1)–O(8)	74.78(8)	O(11)–Dy(1)–O(8)	81.14(9)
O(6)#2–Dy(1)–O(8)	85.94(8)	O(10)–Dy(1)–O(6)#3	96.42(10)
O(2)#1–Dy(1)–O(6)#3	74.55(8)	O(1)–Dy(1)–O(6)#3	75.03(8)
O(11)–Dy(1)–O(6)#3	128.97(8)	O(6)#2–Dy(1)–O(6)#3	74.93(8)
O(8)–Dy(1)–O(6)#3	148.05(8)	O(10)–Dy(1)–O(7)	123.04(10)
O(2)#1–Dy(1)–O(7)	72.26(8)	O(1)–Dy(1)–O(7)	119.31(8)
O(11)–Dy(1)–O(7)	68.66(9)	O(6)#2–Dy(1)–O(7)	75.66(8)
O(8)–Dy(1)–O(7)	52.93(8)	O(6)#3–Dy(1)–O(7)	140.36(8)
O(10)–Dy(1)–O(5)#3	72.55(10)	O(2)#1–Dy(1)–O(5)#3	71.82(9)
O(1)–Dy(1)–O(5)#3	108.65(9)	O(11)–Dy(1)–O(5)#3	77.48(9)
O(6)#2–Dy(1)–O(5)#3	122.34(8)	O(8)–Dy(1)–O(5)#3	151.50(9)
O(6)#3–Dy(1)–O(5)#3	51.91(8)	O(7)–Dy(1)–O(5)#3	132.03(8)

Symmetry transformations used to generate equivalent atoms: #1: $-x+1, -y, -z+1$; #2: $-x+1, -y, -z$; #3: $x, y, z+1$.

Table 3. Bond lengths [Å] and angles [°] for **2**.

Ho(1)–O(4)	2.3540(14)	Ho(1)–O(5)#1	2.3572(14)
Ho(1)–O(9)	2.3959(17)	Ho(1)–O(2)	2.4157(13)
Ho(1)–O(9)#1	2.4820(13)	Ho(1)–O(1)	2.4964(14)
Ho(1)–O(8)	2.5400(14)	Ho(1)–O(10)	2.3862(15)
Ho(1)–O(11)	2.3336(16)		
O(11)–Ho(1)–O(4)	140.14(5)	O(11)–Ho(1)–O(5)#1	69.93(6)
O(4)–Ho(1)–O(5)#1	139.31(5)	O(11)–Ho(1)–O(10)	70.84(6)
O(4)–Ho(1)–O(10)	84.66(5)	O(5)#1–Ho(1)–O(10)	135.90(5)
O(11)–Ho(1)–O(9)	141.74(5)	O(4)–Ho(1)–O(9)	74.43(5)
O(5)#1–Ho(1)–O(9)	71.83(5)	O(10)–Ho(1)–O(9)	142.89(5)
O(11)–Ho(1)–O(2)	82.73(6)	O(4)–Ho(1)–O(2)	125.03(5)
O(5)#1–Ho(1)–O(2)	74.52(5)	O(10)–Ho(1)–O(2)	81.34(6)
O(9)–Ho(1)–O(2)	85.99(5)	O(11)–Ho(1)–O(9)#1	96.53(6)
O(4)–Ho(1)–O(9)#1	74.45(5)	O(5)#1–Ho(1)–O(9)#1	75.36(4)
O(10)–Ho(1)–O(9)#1	128.68(5)	O(9)–Ho(1)–O(9)#1	74.94(5)
O(2)–Ho(1)–O(9)#1	148.14(4)	O(11)–Ho(1)–O(1)	122.93(6)
O(4)–Ho(1)–O(1)	72.23(5)	O(5)#1–Ho(1)–O(1)	119.38(5)
O(10)–Ho(1)–O(1)	68.62(5)	O(9)–Ho(1)–O(1)	75.86(5)
O(2)–Ho(1)–O(1)	53.13(5)	O(9)#1–Ho(1)–O(1)	140.31(4)
O(11)–Ho(1)–O(8)	72.53(6)	O(4)–Ho(1)–O(8)	71.65(5)
O(5)#1–Ho(1)–O(8)	108.85(5)	O(10)–Ho(1)–O(8)	77.20(6)
O(9)–Ho(1)–O(8)	122.39(5)	O(2)–Ho(1)–O(8)	151.40(5)
O(9)#1–Ho(1)–O(8)	51.91(5)	O(1)–Ho(1)–O(8)	131.77(5)

Symmetry transformations used to generate equivalent atoms: #1: $-x+1, -y+1, -z+1$.

from 2.363(3) to 2.546(2) Å with average distance of 2.442 Å, and the Dy1-O(water) distances are 2.340(3) and 2.396(3) Å. The O-Dy-O(carboxyl) bond angles range from 51.91(18) to 151.50(9)°. Two carboxyl groups of hqda link two Dy(III) ions to form a tetradentate coordination mode (Scheme 1(a)); two carboxyl groups of hqda ligand

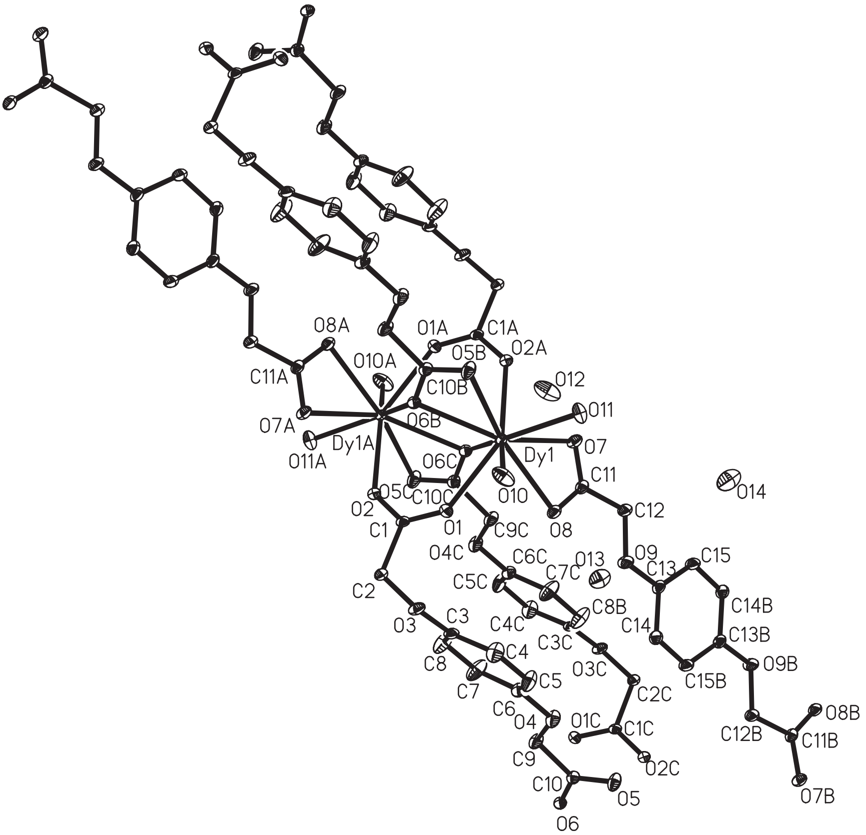

Figure 1. Asymmetric unit of **1** at the 30% probability displacement ellipsoids. All hydrogen atoms are omitted for clarity.

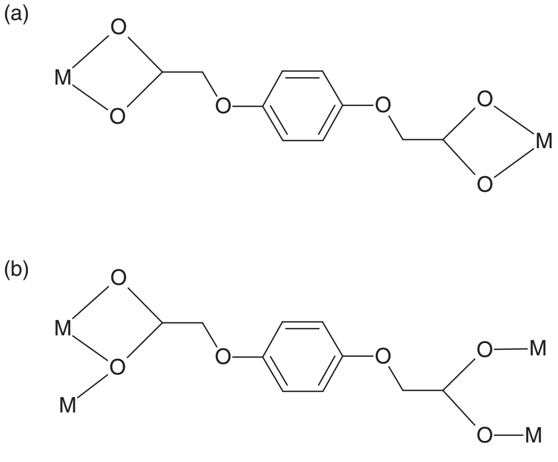

Scheme 1. Coordination modes of hqda ligands.

link four Dy(III) ions in bridging and chelating-bridging modes to form a pentadentate coordination mode (scheme 1(b)). The dimeric unit [$Dy_2(hqda)_3(H_2O)_4$] may be viewed as the building block. Neighboring building blocks are connected through $^{-}OOCCH_2OC_6H_4OCH_2COO^{-}$ ligands to form a 2–D network structure (figure 2).

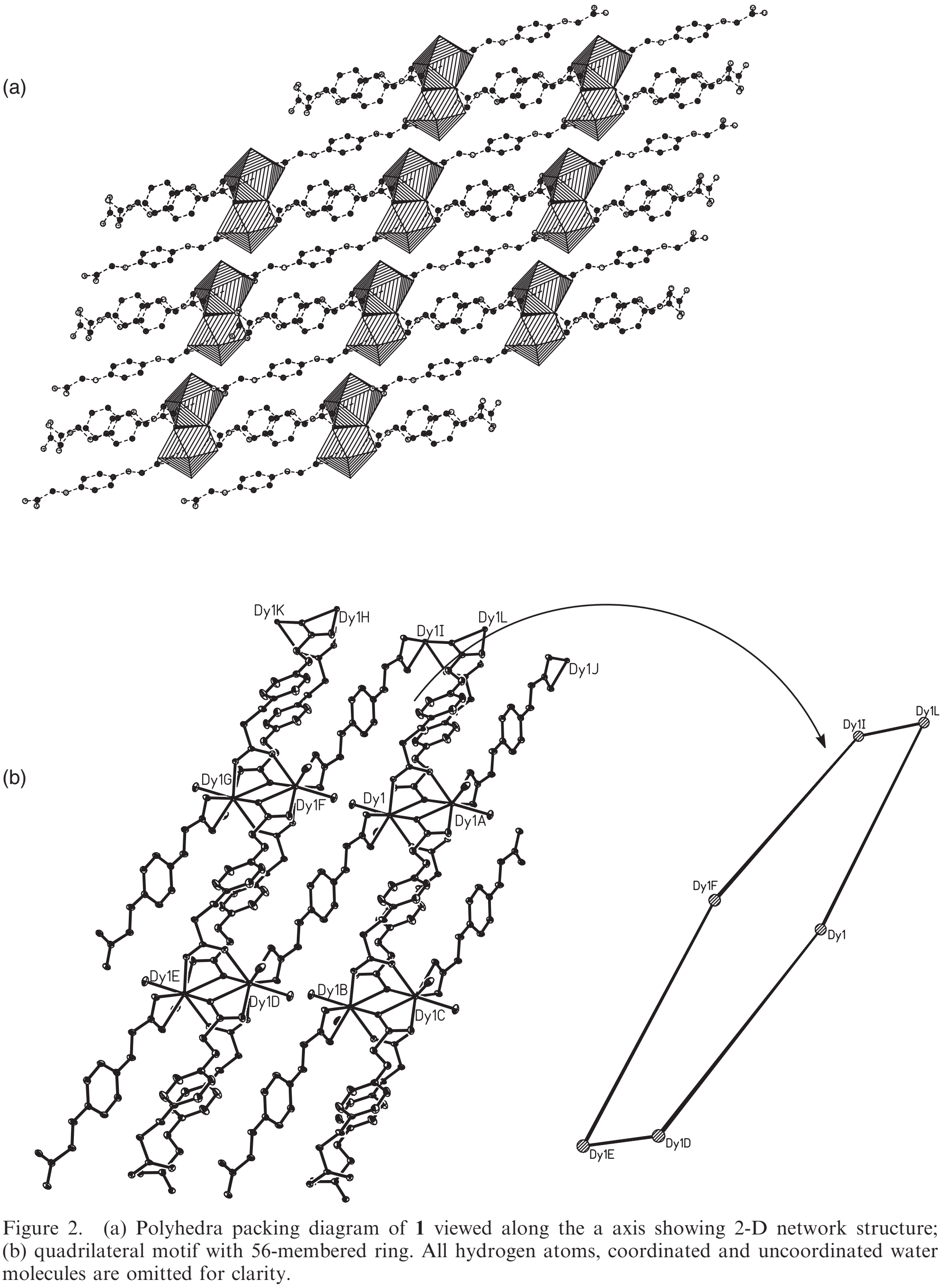

Figure 2. (a) Polyhedra packing diagram of **1** viewed along the a axis showing 2-D network structure; (b) quadrilateral motif with 56-membered ring. All hydrogen atoms, coordinated and uncoordinated water molecules are omitted for clarity.

Six Dy(III) ions build a quadrilateral in which Dy(III) ions are coplanar with no mean deviation from the plane. Four Dy(III) ions occupy four vertexes (Dy1E···Dy1I···Dy1L···Dy1D) of the quadrilateral and the other two ions, Dy1 and Dy1F, locate in the middle of long edges of the quadrilateral. The quadrilaterals have size of 3.885(5) × 29.094 Å based on the Dy···Dy distance. The long edges of the quadrilateral connect two Dy(III) ions through the ($^-$OOCCH$_2$OC$_6$H$_4$OCH$_2$COO$^-$)Dy($^-$OOCCH$_2$OC$_6$H$_4$OCH$_2$COO$^-$) spacers. 2{[Dy(COO$^-$)Dy][($^-$OOCCH$_2$OC$_6$H$_4$OCH$_2$COO$^-$)Dy($^-$OOCCH$_2$OC$_6$H$_4$OCH$_2$COO$^-$)]} form a quadrilateral with a 56-membered ring (figure 2b).

Uncoordinated water molecules (O12, O13, and O14) exist in the crystal lattice and number of hydrogen bonds are formed among the uncoordinated water, carboxylate group oxygen atoms, and coordinated water. Distances of the hydrogen bonds are in the range 2.640–3.090 Å and O···H–O angles are in the range 135.39–177.83° (table 4), which suggest strong hydrogen bonds, further increasing the stability of the structure. Adjacent 2-D layers are interlinked by these hydrogen bonds to form a 3-D supermolecular structure viewed along the *c*-axis, as shown in figure 3.

The complex $\{[Ho_2(hqda)_3(H_2O)_4]\cdot 6H_2O\}_n$ (**2**) is isomorphous with **1**. The building block of **2** containing two Ho(III) ions is shown in figure 4. The two Ho(III) ions in one building block are bridged by carboxylate groups from hqda anions in bidentate-bridging and chelating-bridging modes. The distance between two Ho(III) ions is 3.8718(13) Å. Hqda ligands link these building blocks via chelating/chelating and bridging/chelating-bridging modes to form the 2–D network. A comparison of crystal data between **2** and **1** shows that the average distances of Ho1–O(carboxyl) (2.4340 Å) and Ho1–O(water) (2.3599 Å) in **2** are slightly shorter than those of Dy1–O(carboxyl) and Dy1–O(water) in **1** in accordance with the effect of lanthanide contraction.

Structures of the two title complexes are different from the reported complexes $[Eu_2(1,4\text{-BDOA})_3(H_2O)_2]\cdot 2H_2O$ and $[Er_2(1,4\text{-BDOA})_3(H_2O)_2]$ (1,4-BDOA = hydroquinone-O,O′-diacetic acid) [12], which were prepared by hydrothermal reaction. In these two complexes ether oxygen atoms from 1,4-BDOA also coordinate lanthanide to form a 2-D network structure different from the title complexes. The title complexes obtained from solution reaction contain more lattice water molecules in the crystal lattice than those under hydrothermal conditions. The various hydrogen bonds result in structural stability and a 3-D framework.

Table 4. Hydrogen bonds (D–H···A) for **1** [Å and °].

D–H	d(D–H)	d(H···A)	∠DHA	d(D···A)	A
O10–H10A	0.848	1.798	171.68	2.640	O12 [x + 1, y, z]
O10–H10B	0.848	1.883	170.38	2.722	O13 [−x + 2, −y + 1, −z + 1]
O11–H11A	0.848	1.915	163.08	2.737	O13 [−x + 2, −y + 1, −z + 1]
O11–H11B	0.849	2.039	168.64	2.877	O7 [−x + 1, −y + 1, −z + 1]
O12–H12A	0.854	2.017	154.36	2.811	O3 [x − 1, y, z]
O12–H12B	0.850	2.114	147.96	2.870	O7
O13–H13A	0.850	1.954	166.03	2.786	O14 [x + 1, y, z]
O13–H13B	0.850	1.943	177.83	2.793	O8
O14–H14A	0.845	2.108	152.02	2.882	O5 [−x + 1, −y + 1, −z]
O14–H14A	0.845	2.431	135.39	3.090	O4 [−x + 1, −y + 1, −z]

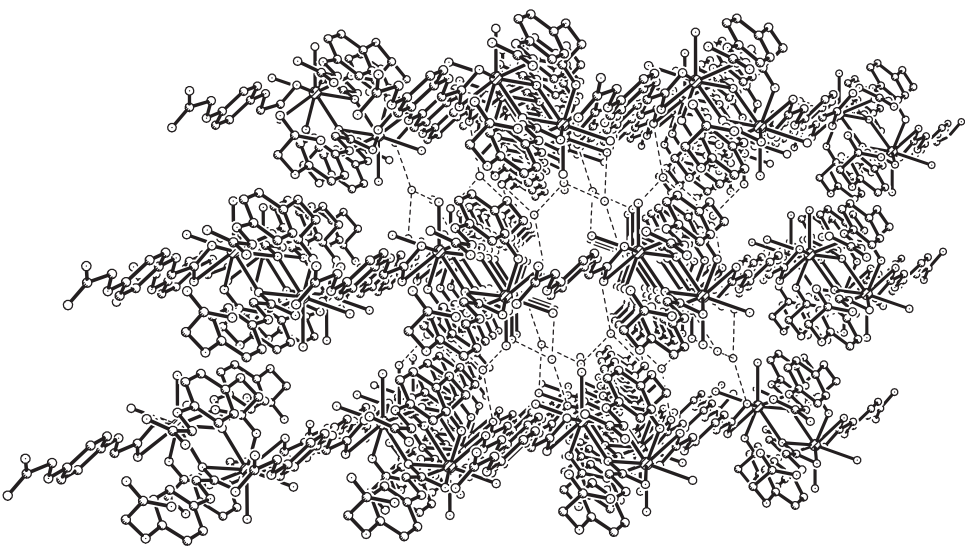

Figure 3. Packing diagram of **1** viewed along the c-axis showing the H-bonding interactions.

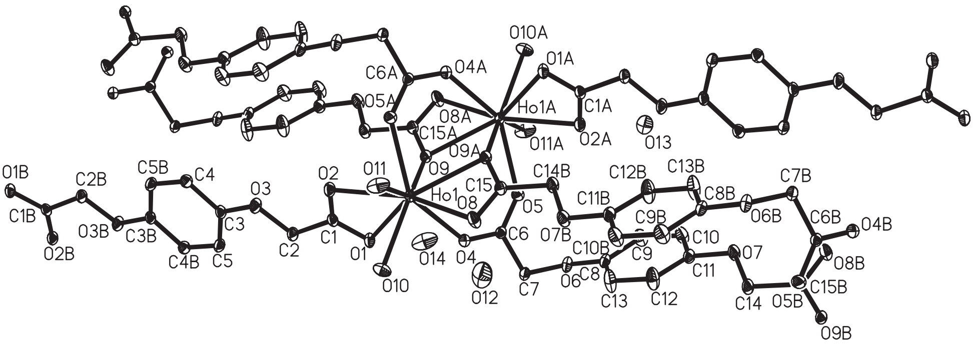

Figure 4. Asymmetric unit of **2** at the 30% probability displacement ellipsoids. All hydrogen atoms are omitted for clarity.

3.2. *Fluorescence spectrum*

The excitation spectrum was recorded from 200 to 400 nm with the emission wavelength of 481 nm. Fluorescence was observed in the range 400–600 nm by selective excitation wavelength of 309 nm, as shown in figure 5. There are two main emission peaks in the luminescence spectrum, 481 and 573 nm, corresponding to the transitions between the first excited state ($^4F_{9/2}$) and the ground-state multiplet ($^6H_{15/2\text{-}13/2}$) of the Dy(III) ion, namely the $^4F_{9/2} \rightarrow {}^6H_{15/2}$, $^4F_{9/2} \rightarrow {}^6H_{13/2}$ transitions of Dy(III), respectively.

3.3. *Thermogravimetric analysis*

The DTA-TG analysis was studied in air with a heating rate of 10°C min^{-1} from 20 to 1000°C. The DTA-TG curves of the two complexes are similar. There are small

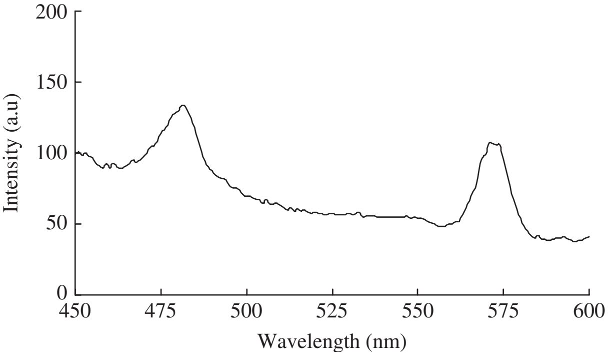

Figure 5. The fluorescence spectrum of **1** ($\lambda_{ex} = 309$ nm).

endothermic peaks at 103 and 180°C for **1**, 108 and 189°C for **2**, which are caused by the release of all crystal and coordination water molecules. The corresponding weight loss is 15.68% (calculated, 15.28%) for **1** and 15.40% (calculated, 15.22%) for **2**, respectively. Finally, there are strong exothermic peaks at 394°C for **1** and 386°C for **2**. The final residues are oxides Dy_2O_3 for **1** and Ho_2O_3 for **2**, corresponding to the total loss of 68.05% (calculated, 68.32%) for **1** and 66.11% (calculated, 68.04%) for **2**.

Supplementary material

CCDC-645551 for **1** and 645552 for **2** contain the supplementary crystallographic data for this paper. These data can be obtained free of charge from CCDC, 12 Union Road, Cambridge, CB2 1EZ, UK (Fax: +44(0)1223-336033; Email: deposit@ccdc.cam.ac.uk).

Acknowledgements

We are grateful to the Natural Science Foundation of Beijing (No. 2073022), the Scientific Research Common Program of Beijing Municipal Commission of Education, and the Young Mainstay Teachers Foundation of Beijing Municipal Universities

References

[1] B.D. Chandler, D.T. Cramb, G.K.H. Shimizu. *J. Am. Chem. Soc.*, **128**, 10403 (2006).
[2] I. Kumagai, M. Akita-Tanaka, K. Inoue, M. Kurmoo. *J. Mater. Chem.*, **11**, 2146 (2001).
[3] A. Figuerola, J. Ribas, D. Casanova, M. Maestro, S. Alvarez, C. Diaz. *Inorg. Chem.*, **44**, 6949 (2005).
[4] A.G. Wong-Foy, A.J. Matzger, O.M. Yaghi. *J. Am. Chem. Soc.*, **128**, 3494 (2006).
[5] L. Pan, K.M. Adams, H.E. Hernandez, X. Wang, C. Zheng, Y. Hattori, K. Kaneko. *J. Am. Chem. Soc.*, **125**, 3062 (2003).
[6] T.M. Reineke, M. Eddaoudi, M. Fehr, D. Kelley, O.M. Yaghi. *J. Am. Chem. Soc.*, **121**, 1651 (1999).
[7] Y.H. Wan, L.P. Jin, K.Z. Wang, L.P. Zhang, X.J. Zheng, S.Z. Lu. *New J. Chem.*, **26**, 1590 (2002).

[8] C. Daiquebonne, N. Kerbellec, K. Bernot, Y. Gérault, A. Deluzet, O. Guillou. *Inorg. Chem.*, **45**, 5399 (2006).

[9] X.J. Zheng, T.T. Zheng, L.P. Jin. *J. Mol. Struct.*, **740**, 31 (2005).

[10] C. Serre, F. Millange, J. Marrot, G. Férey. *Chem. Mater.*, **14**, 2409 (2002).

[11] A. Deluzet, W. Maudez, C. Daiguebonne, O. Guillou. *Cryst. Growth Des.*, **3**, 475 (2003).

[12] X.F. Li, Z.B. Han, X.N. Cheng, X.M. Chen. *Inorg. Chem. Commun.*, **9**, 1091 (2006).

[13] Y. Yang, G.Q. Jiang, Y.Z. Li, J.F. Bai, Y. Pan, X.Z. You. *Inorg. Chim. Acta*, **359**, 3257 (2006).

[14] S. Gao, J.W. Liu, L.H. Huo, Y.M. Xu, H. Zhao. *Inorg. Chem. Commun.*, **8**, 361 (2005).

[15] G.M. Sheldrick. *Acta Cryst.*, **A46**, 467 (1990).

[16] G.M. Sheldrick. *SHELXL97, Program for X-ray Crystal Structure Solution*, University of Göttingen, Germany (1997).